

low-frequency band, 80–320 Hz for the midfrequency band, and 320–1000 Hz for the high-frequency band.

After filtering, the video signal was passed through a threshold detector and a pulse generator that generated a pulse as the signal level exceeded the preselected threshold and terminated the pulse as the signal decayed below this threshold. This signal triggered a 2-kHz pulse generator to detect large areas of contrast. This high-frequency modulation is necessary because the unmodulated signal would be counted as a single point of contrast with no consideration given to the pulse width (i.e., large obstacles or slopes). The digital counter counts the pulses, which are a direct measure of surface roughness. The count is displayed on an electronic counter for each bandwidth.

#### Experimental Results

A typical experiment consisted of scanning a boulder field at medium altitude, followed by a low-altitude scan, centered on the area with the best figure of merit as determined by the scan at medium altitude. A photograph of the lunar surface containing a dense distribution of rocks and boulders was selected to provide maximum strain on the breadboard system's ability to locate a relatively smooth area. The camera was electronically aimed so the instantaneous  $12^\circ$  FOV was approximately centered on the photograph (Fig. 7). Again, each figure of merit was determined by scanning a  $2 \times 2$  in. area.

The larger area scanned contains the figures of merit obtained using the modulated midfrequency signal. A desirable landing area is not obvious from the photograph because of the high density of rocks and boulders. Closer visual examination of the scanned surface areas verifies that the middle and lower-middle areas contain a lower density of rocks and boulders, as indicated by the respective figures of merit. The lower-middle area was identified by the breadboard system as the best area by all frequency bands. The camera's instantaneous FOV was then aimed electronically at the center of the lower-middle area and the zoom lens adjusted to reduce the size of the area to be scanned to  $1 \times 1$  in., thus simulating a decreased altitude. The area scanned is outlined by the smaller squares, which also contain figures of merit generated by the midfrequency band signal. The reduced size of the area of scan introduces the influence of smaller rocks on the figures of merit, and increases the relative influence of the rocks and boulders picked up by the scan at the higher altitude. The best landing site identified by the midfrequency signal can be visually verified by noting a relatively smaller density of obstacles in this region. The dynamic response of the system, which would produce another steering decision from a reduced FOV, would isolate the obstacles identified in the low-frequency channel and would avoid them as long as a smooth area is indicated.

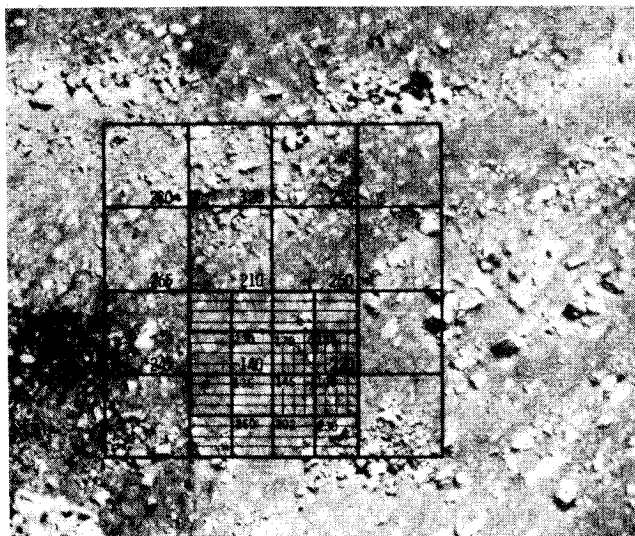


Fig. 7 Simulated site selection.

#### Conclusions

The feasibility of a PLS<sup>3</sup> has been established. State-of-the-art miniature hardware available for the Viking mission could result in a very lightweight, sterilizable system. For every surface generated in the simulations, the lander found a smooth area and executed a successful landing. Analysis of the results indicates that a PLS<sup>3</sup> requiring minimal interface with the lander, negligible additional fuel, and minimal additional flight computer software can be built. In every case, the breadboard system identified a desirable landing area. The important conclusion from breadboard testing is that the desired surface information is present in the raw camera signal and can be extracted. It is concluded that a PLS<sup>3</sup> could provide greater mission flexibility and could be adapted to future missions with a minimum effect on the present Viking lander configuration.

## Detection of Flight Vehicle Transition from Base Measurements

BRUCE M. BULMER\*

Sandia Laboratories, Albuquerque, N. Mex.

#### Introduction

THE prediction of boundary-layer transition on full-scale conical re-entry vehicles (RV's) in ballistic flight is a necessary and important part of preflight design analyses. Empirical prediction techniques inherently must rely upon flight transition data obtained from vehicles having similar configurations and heatshield ablation characteristics. While it is usually advantageous to have complete instrumentation onboard a vehicle to detect the onset of transition, most RV's use ablative heatshields for high-performance flight. As a result, complete heatshield instrumentation (particularly for RV frustum surface temperature, which is probably the best indication of transition) is often impractical and in some instances impossible.

In contrast, base data measurements are generally very easy to obtain because the thermal environment in the base-flow region is far less severe than on the frustum preceding the base. Therefore, instrumentation problems associated with the extreme thermal environment on the frustum are almost entirely eliminated on the base. Base pressure and heat-transfer measurements provide extremely useful sources of transition data because the characteristics of base flow are highly dependent upon the upstream boundary-layer condition on the frustum immediately preceding the base (for examples, see Cassanto, Rasmussen, and Coats<sup>1</sup>). As a result, changes in the upstream boundary-layer condition that result from transition onset are immediately detected by the base instrumentation. This Note presents base pressure and heat-transfer data from two RV flight tests that provide very distinct indications of transition onset. These transition indicators are compared with several other indicators for each flight.

Received September 13, 1972; revision received November 27, 1972. This work was supported by the U.S. Atomic Energy Commission.

Index categories: Re-Entry Vehicle Testing; Boundary-Layer Stability and Transition; Jets, Wakes, and Viscid-Inviscid Flow Interactions.

\* Member, Technical Staff, Re-Entry Vehicle Aerothermodynamics Division. Member AIAA.

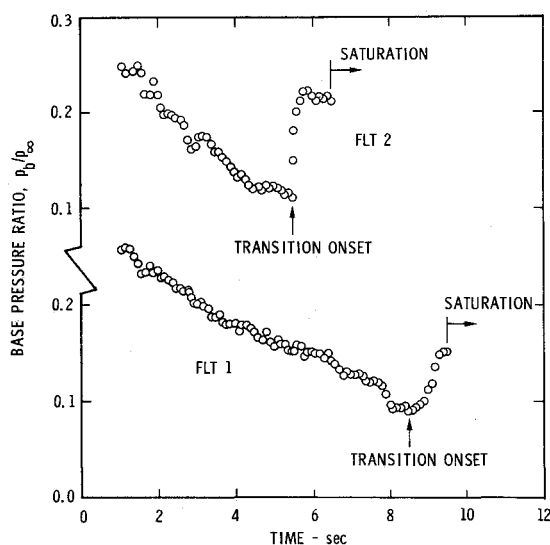


Fig. 1 Flight test base pressure data.

### Discussion

Base measurements on two slender, slightly blunted RV's having approximately flat base geometry were obtained from a pressure transducer (0–1 psia range) and a calorimeter (0–120 Btu/ft<sup>2</sup>-sec range) mounted near the centerline of each vehicle. The transducers had a short pneumatic system (tube length/port diameter ratio of 40) so that the pressure time lag was negligible in the altitude range of interest, and the calorimeters were mounted flush with the base cover to insure good response and accuracy. The pressure and heat flux were telemetered at 15 samples per second.

In addition to the base measurements, transition data were obtained from accelerometers, frustum heatshield thermocouples just forward of the base, and offboard optical instrumentation (both aircraft- and ground-based). Flight 2 was also instrumented for lateral vibration.

The base pressure and heat-transfer data (Figs. 1 and 2) show

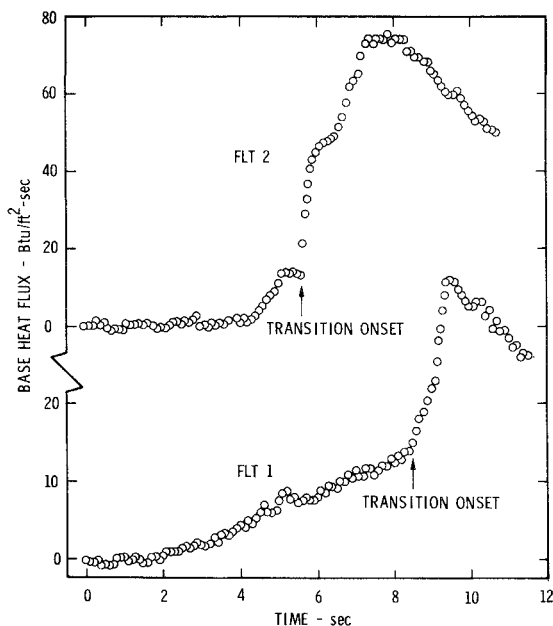


Fig. 2 Flight test base heat-transfer data.

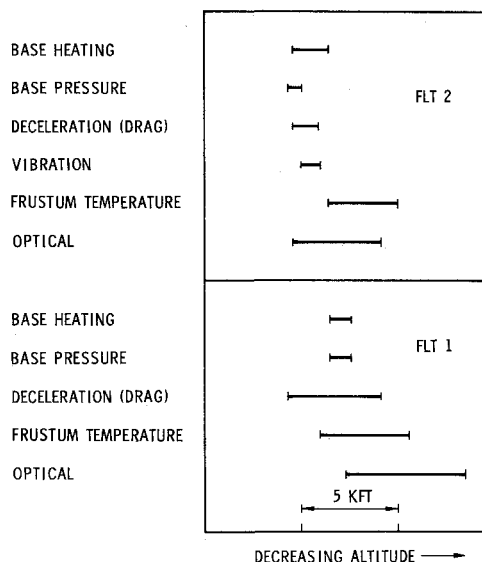


Fig. 3 Flight results: transition indicator summaries.

the typical effect of transition on slender, slightly blunted RV's; that is, the distinct minimum in the base pressure ratio ( $p_b/p_\infty$ ) history and the sharp increase in the base heat flux history are indicative of transition onset on the frustum immediately preceding the base. These data provide distinct indications of transition onset because changes occur over relatively short time intervals (one or two tenths of a second). In addition, one may readily detect changes in the raw data without resorting to further data reduction or manipulation.

The base pressure and heat-transfer transition data are compared with other transition indicators in Fig. 3. The interpretation of these other indicators follows that of Sherman and Nakamura.<sup>2</sup> Each indicator's altitude spread reflects the uncertainty in determining transition onset from that particular piece of data. For both flights, the base indicators agree very well with the accelerometer and vibration data, and good agreement with the frustum heatshield temperature data, measured just forward of the base, is also noted. The optical data indicate transition onset at a slightly lower altitude than do the base data. The optical data were obtained from offboard instrumentation and reveal increased heating along the RV frustum associated with the movement of transition over a portion of the vehicle. Hence, these data, while providing an independent verification of the transition altitude, are expected to indicate transition onset at a slightly lower altitude than do the base data.

The good agreement seen among the transition data in Fig. 3 illustrates the utility of base pressure and heat-transfer data as indicators of transition onset on full-scale vehicles during re-entry. For both flights, the base data fall well within the altitude band of the other indicators (~10 kft for Flight 1 and ~6 kft for Flight 2) and in general represent some of the earliest (i.e., highest-altitude) indications of transition onset on the vehicles. While these results are restricted to RV's with approximately flat base geometry, it is concluded that base pressure and heat-transfer measurements provide, within an accuracy of a few kft altitude, reliable and easy-to-obtain ballistic re-entry transition data.

### References

- 1 Cassanto, J. M., Rasmussen, N. S., and Coats, J. D., "Correlation of Free-Flight Base Pressure Data for  $M = 4$  to  $M = 19$ ," *AIAA Journal*, Vol. 7, No. 6, June 1969, pp. 1154–1157.
- 2 Sherman, M. M. and Nakamura, T., "Flight Test Measurements of Boundary-Layer Transition on a Nonablating 22° Cone," *Journal of Spacecraft and Rockets*, Vol. 7, No. 2, Feb. 1970, pp. 137–142.